Biophysics and Physicobiology

Regular Article

Development of the force field for cyclosporine A

Tsutomu Yamane[1,2], Toru Ekimoto[1], Mitsunori Ikeguchi[1,2]

[1] *Graduate School of Medical Life Science, Yokohama City University, Yokohama, Kanagawa 230-0045, Japan*
[2] *HPC- and AI-driven Drug Development Platform Division, Center for Computational Science, RIKEN, Yokohama, Kanagawa 230-0045, Japan*

Membrane permeability of cyclic peptides is an important factor in drug design. To investigate the membrane permeability of cyclic peptides using molecular dynamics (MD) simulations, the accurate force fields for unnatural amino acids present in the cyclic peptides are required. Therefore, we developed the CHARMM force fields of the unnatural amino acids present in cyclosporin A (CsA), a cyclic peptide used as an immune suppressor. Especially for N-methyl amino acids, which contribute to the membrane permeability of cyclic peptides, we developed a grid correction map (CMAP) of the energy surface using the φ and ψ dihedral angles in the main chain of CsA. To validate the developed force field, we performed MD simulations, including the generalized replica exchange with solute tempering method, of CsA in water and chloroform solvents. The conformations of CsA in water and chloroform sampled using the developed force field were consistent with those of the experimental results of the solution nuclear magnetic resonance spectroscopy.

◀ *Significance* ▶

Cyclic peptides, as middle molecular weight drugs, have received considerable attention in drug development. Because of the flexibility of cyclic peptides, molecular dynamics simulations would be useful for investigating their dynamic properties such as membrane permeability. An accurate force field for cyclic peptides is required to perform molecular dynamics simulations; therefore, we developed the CHARMM force field for unnatural amino acids in a representative cyclic peptide, cyclosporin A. Results simulated using the developed CHARMM force field were consistent with experimental data such as those of nuclear magnetic resonance spectroscopy.

Introduction

Recently, middle-molecular-weight drugs (500–2,000 Da), which are between the conventional low- and high-molecular-weight drugs (e.g., antibodies), have attracted much attention in drug development [1]. These drugs have the ability to cross cell membranes, similar to low-molecular-weight drugs, and inhibit protein–protein interactions, similar to high-molecular-weight drugs [1]; these drugs may, therefore, inhibit protein–protein interactions inside cells.

Cyclosporin A (CsA) is one of the most successful drugs among the conventional low- and high-molecular weight drugs. CsA is a cyclic undecapeptide with a molecular weight of 1,202.6 Da (Figure 1A), and is used as an immunosuppressant [2-4]. The immunosuppressive effect of CsA arises from its capacity to inhibit signal transduction of the immune response

Corresponding author: Mitsunori Ikeguchi, Graduate School of Medical Life Science, Yokohama City University, 1-7-29, Suehiro-cho, Tsurumi-ku, Yokohama, Kanagawa 230-0045, Japan. ORCID iD: https://orcid.org/0000-0003-3199-6931, e-mail: ike@yokohama-cu.ac.jp

by binding to cyclophilin (CyP) in the T cells [5,6]. The remarkable feature of CsA is its high membrane permeability despite its high molecular weight. The three-dimensional structure of CsA has been investigated to elucidate the molecular mechanism underlying its cell membrane permeability [7-12]. In the crystal structure, CsA adopts two forms: closed and open (Figure 1B and 1C). The open form was observed in the crystal structure of CsA complexed with CyP [7]. In the open form, no intramolecular hydrogen bonds are found, and polar groups are exposed to the solvent. Therefore, the open form appears to be hydrophilic and stable in water [8-10]. In contrast, the closed form is observed in the crystal structure of CsA in chloroform [12]. The closed form has four intramolecular hydrogen bonds (Figure 1B), and the polar groups face inwards in the molecule. Thus, the closed conformation appears to be stable in a hydrophobic environment (e.g., within cell membranes). It is hypothesized that structural transition between the open and closed forms occurs during permeation across membranes [13,14], and CsA adopts the open form in water. CsA undergoes conformational changes upon entering the cell membrane and assumes the closed form; further, it changes its conformation back to the open form upon crossing the membrane. It is noteworthy that the dihedral angle of the peptide bond (ω) between two unnatural amino acids in CsA, MLE2 and MLE3, is different in the open and closed forms. In the open form, the ω angle is 180° (*trans*), whereas in the closed form, the ω angle is 0° (*cis*) (Figure 1B and 1C).
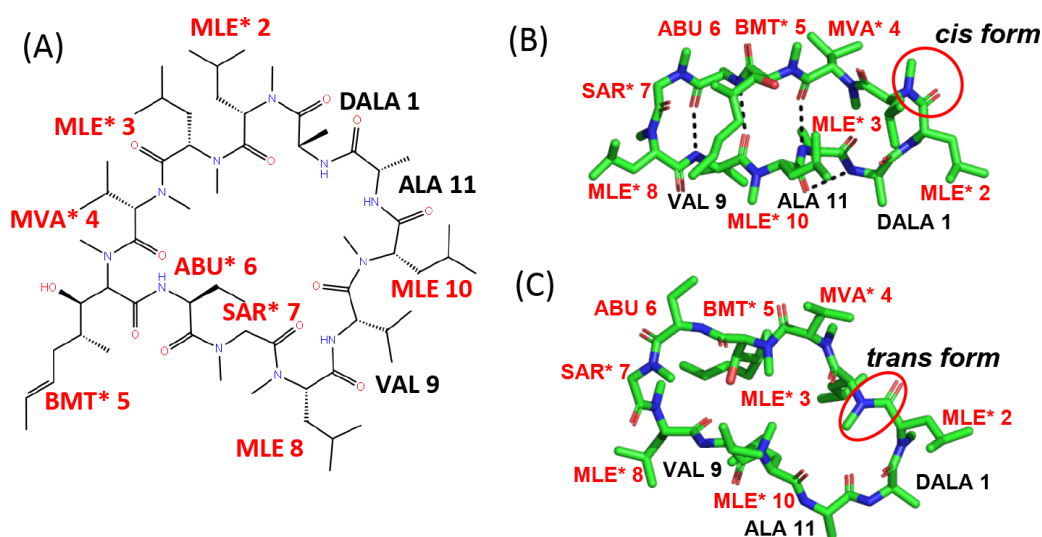

Figure 1 Structures of cyclosporin A. (A) The chemical structural formula of cyclosporin A. (B) The crystal structure of the closed form of cyclosporin A from Cambridge structural database (CSD) [CDC ID: DEKSAN]. Black dotted line represents hydrogen bonds. (C) The crystal structure of the open form of cyclosporin A [PDB ID: 1CWA]. Unnatural amino acids residues are labelled in red and residue names of N-methyl amino acids are followed by an asterisk. In panels (B) and (C), ω angles between MLE2 and MLE3 are depicted in red circles. All graphical depictions of 3D structures in this paper were generated using the program PyMOL [15].

N-methylation in the backbone of cyclic peptides is crucial for their membrane permeation [5-14,16-20]. In CsA, seven out of 11 residues are N-methylated. Because N-methylation inhibits the hydrogen-bonding ability of amino groups, the closed form, in which N-methyl groups are exposed to the solvent, hydrogen bond formation with solvent molecules is difficult. Therefore, the closed form of CsA prefers hydrophobic environment. Furthermore, according to quantum mechanics (QM) calculations, the energy barrier between the *cis* and *trans* states of the ω angle between the two N-methyl amino acids is smaller than that of natural amino acids [21]. Thus, the *cis–trans* transition of the dihedral angle ω between the two N-methyl amino acids is more likely to occur than in natural amino acids.

The structural dynamics of CsA, cyclic peptides, and small drugs during membrane permeability have been studied using molecular dynamics (MD) simulations [13,14,22-27]. Witek et al. examined stable conformations of CsA [13], its metabolite, cyclosporin E, and cyclic decapeptides in water or chloroform, and showed structural ensemble models given by the Markov state model (MSM) integrating multiple short MD simulations with the GROMOS force field [24,25]. Ono et al. performed multi-canonical MD simulations of CsA in various solvents, such as water and chloroform, using different AMBER force fields, and examined the performance of the force fields by comparing the sampled conformational ensemble with experimental data [26]. The membrane permeability of CsA, cyclic peptides, and small compounds were examined using high-temperature MD with a CHARMM force field [14], replica exchange MD with AMBER force field [27], or potential mean force analysis by short MD simulations with AMBER force field using membrane-water systems

[23]. These studies suggest that the structural features vary during translocation across the membrane, corresponding to the hydrophilic and hydrophobic environments and their interfaces. However, it was also suggested that the conformational sampling strongly depended on the accuracy of the force field and the extent of sampling. In particular, the performance of the force field of not only the molecules that permeate the membrane but also the membrane molecules is an important aspect of simulating membrane permeation [22].

For plausible MD simulations of CsA, an accurate force field including N-methyl amino acids is required. In the recent CHARMM force field for proteins, the grid correction map (CMAP) term, which is a correction for potential-energy cross terms of backbone dihedral angle ϕ and ψ, improves the accuracy of backbone conformations of natural amino acids [28]. However, the CMAP terms for N-methyl amino acids have not yet been developed. In recent years, a CHARMM force field without CMAP terms has been developed for peptoids, whose residues are analogs of N-methyl amino acids [29,30]. In peptoids, side chains are connected to the nitrogen atoms of the backbone rather than to the α-carbons. In CsA, a sarcosine residue (N-methyl glycine) is a peptoid residue.

In this study, we developed the CHARMM force field for CsA, including the CMAP terms of N-methyl amino acids, and MD simulations of CsA in water and chloroform were performed to verify the validity of the force field. Because the timescale of *cis–trans* transitions of the ω angle exceeds the timescale of current conventional MD simulations (~µs), in this study, we employed the generalized replica exchange with solute tempering (gREST) method, which is an extended ensemble method [31]. Using the gREST method, the conformational changes that cross a high-energy barrier can be sampled efficiently.

This study might provide valuable insights regarding the force fields for peptides.

Methods

Development of the CHARMM Force Field for Cyclosporin A

In this study, we developed the CHARMM force field for unnatural amino acids, MLE, MVA, BMT, ABU, and SAR, which are represented by red letters in Figure 1A. The atom types in these residues were chosen mainly from the topology files of the CHARMM36 force field (top_all36_carb.rtf, top_all36_cgennff.rtf, and top_all36_prot.rtf) [32]. The partial atomic charges of these residues were determined with reference to the charges of amino acids and small molecules in CHARMM36. For the parameters of those residues missing in CHARMM36, the CHARMM generalized force field (CGenFF) for N-methyl alanine dipeptide was used [33-37]. The parameter sets and topology files developed in this study are available at github.com/IkeguchiLab/CsA_FF.

Calculation of the CMAP Terms of N-methyl Amino Acids

The CMAP terms of N-methyl amino acids were calculated using the same procedure as that employed in the CHARMM36 study for natural amino acids [32]. Here, we calculated the CMAP terms of the N-methyl alanine and N-methyl glycine (sarcosine) dipeptide models. For comparison, the CMAP terms of alanine and glycine were calculated. The backbone torsion angles of these dipeptide models (ϕ, ψ) were rotated by 15° and 576 conformations were generated. These structures were optimized using the MP2/aug-cc-pVDZ level using Gaussian09 [38]. Next, single-point energies were calculated for the optimized structures using the RIMP2/cc-pVTZ and RIMP2/cc-pVQZ levels by QCHEM ver. 5.0.2 [39]. From these results, the single-point energies with the complete basis set were calculated using the method of Halkier et al. [40].

The main chain (ϕ, ψ) conformational energy maps, E (ϕ, ψ), for four dipeptide models of amino acids (N-methyl alanine, N-methyl glycine [sarcosine], alanine, and glycine) were obtained from high-precision QM calculations (RIMP2/CBS//MP2/aug-cc-pVDZ) (Figure 2A–D). The energy of the CHARMM force field was corrected using the CMAP terms to reproduce the QM energy maps, E (ϕ, ψ).

Conformational Sampling using the gREST Method

The gREST method is an improved version of the replica exchange with solute tempering (REST) method [41]. In the standard replica exchange method, for the enhancement of conformational sampling, the exchange of the system temperature between replicas is attempted using the Metropolis criteria every several time steps [41]. However, when the system is large (e.g., with many solvent molecules), the system temperatures hardly change because of small fluctuations in the system energy. In REST, the temperatures of only the "solutes" are exchanged to overcome this problem [41]. Using REST, one can achieve a sufficient exchange ratio of solute temperatures, even for large systems. In REST2, the energy terms involving a solute are scaled instead of heating the solute to improve efficiency [42]. In gREST, which is a generalized version of REST2, the scaled energy terms can be chosen from the energy terms defined in the force field [31].

The gREST simulations were performed for CsA in water and chloroform using GENESIS ver. 1.3.0 [43,44]. Here, CsA was defined as a solute, and the dihedral angle and CMAP terms were scaled in 10 replicas corresponding to 10

temperatures, 300 K, 305 K, 315 K, 330 K, 350 K, 375 K, 405 K, 440 K, 480 K, and 525 K. All the bonds that involved hydrogen atoms were constrained using the SHAKE algorithm, and the integration time step was 2 fs. The long-range electrostatic interactions were calculated using the particle mesh Ewald method. The CHARMM-GUI [45,46] was used for the setup of the water and chloroform systems. The CHARMM36m force field was used for normal amino acids and d-alanine in CsA [47]. Water and chloroform solvent systems were constructed in a box cell (50×50×50 Å). The TIP3P model was used for water [48], Dietz and Heinzinger model was used for the partial atomic charges, and Lennard Jones parameters was used for kit modules chloroform [49]. Other force field parameters of chloroform were determined using the Gaussian09 and force field tool of VMD [50]. In the 100 ns MD simulation for pure chloroform using this force field at 300 K and 1 atm, the average density was 1.46 g/cm^3, which was close to the experimental value (1.48 g/cm^3). The closed crystal structure [CDC ID: DEKSAN] was used as the initial structure for the gREST simulations. Before the production run, we performed a 1 ns equilibration run in the NPT ensemble for each of the 10 replicates. Then, the 500 ns production run was carried out using the gREST method. The exchange of solute temperatures of the replicas was attempted every 1,000 steps. A series of simulations were performed with and without the CMAP terms in water and chloroform (total simulation time was 20 μs). After the production run, all flames at 300 K were extracted from the trajectories and used for analysis.

Molecular Dynamics Simulations of CsA

For comparison, we performed conventional MD simulations of CsA in water using the developed force field with GROMACS 2016.3 [51]. The crystal structures of the open form [PDB ID: 1CWA] and closed form [CDC ID: DEKSAN] were used as the initial structures [7,12]. The conditions of the MD simulations were the same as those used in the gREST simulations in water. The MD simulations from the open and closed initial structures were performed for 1 μs each at 300 K and 1 atm.

Principal Component Analysis

For analysis of trajectories, we performed principal component analysis (PCA) using Cα coordinates of CsA. The principal component (PC) axes were determined using the trajectories of the conventional MD simulations from the open and closed forms of CsA in water. Snapshots of the trajectories of the gREST simulations and conventional MD simulations were projected onto a plane constructed using the first and second PCs. The probabilities of the snapshots on the plane were obtained and converted to free energies.

Results and Discussion

Energy Maps of Dipeptide Models

The energy landscapes of the N-methyl dipeptide models were different from those of normal amino acids. In particular, the energy barriers in the two regions around (ϕ, ψ) = (150°, 45°) and (165°, −165°) were observed only in the N-methyl amino acids (regions A and B in Figure 2A and 2B). The energy barriers are due to the steric repulsion of the bulky methyl group attached to the amide group (Figure 2E and 2F). In contrast, in natural amino acids, hydrogen bonds between the amide proton and carbonyl oxygen can be formed. The energy map of the dipeptide model of the natural amino acids has three minima (C7eq, C7ax, and C5) (Figure 2) [52]. However, in the dipeptide model of the N-methyl amino acids, the minimum C5 around (ϕ, ψ) = (−150°, 150°) was not observed. This is also due to the steric repulsion of the N-methyl groups, as discussed previously.

The (ϕ, ψ) conformations of N-methyl amino acids in the open and closed crystal structures of CsA were distributed around the stable regions of the energy maps of N-methyl alanine (Figure 3A) and N-methyl glycine (Figure 3B) obtained in this study, suggesting that the energy map reproduces the actual backbone stability of N-methyl amino acids. The conformations sampled in the MD simulations appear according to the energy maps. Therefore, conformational sampling without CMAP is inappropriate because the conformations in regions A and B can appear frequently.

gREST Simulations for CsA in Chloroform

We performed gREST simulations of CsA in chloroform using the CHARMM force field with and without the CMAP terms for N-methyl amino acids developed in this study, which are referred to as chcl3-w-CMAP and chcl3-wo-CMAP, respectively.

The sampled conformations projected onto the PCA space (PC1-PC2) chcl3-w-CMAP and chcl3-wo-CMAP were compared (Figure 4A and 4B). In the free-energy landscape of chcl3-w-CMAP, all conformations were distributed around the closed crystal structure [CDC ID: DEKSAN] (Figure 4A and Figure S9), suggesting two possibilities: (i) the closed structure of CsA was more stable than the open structure in chloroform, or (ii) the initial conformation of CsA was trapped around the closed structure. However, as shown in the next section, gREST simulations in water using the CHARMM
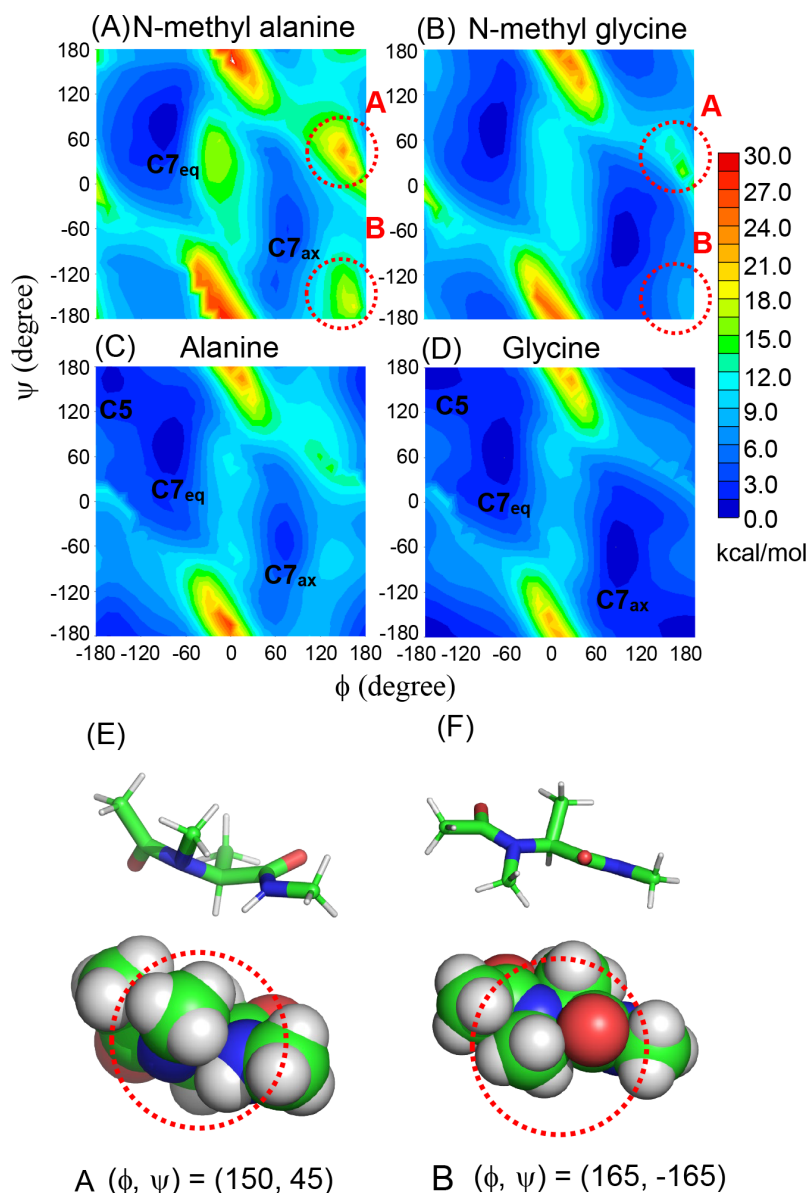
Figure 2 The (ϕ, ψ) energy surfaces of the CHARMM force field with the CMAP term of the dipeptide models of N-methyl alanine (A), N-methyl glycine (Sarcosine) (B), alanine (C), and glycine (D). In panels (A) and (B), energy barriers A and B, which are unique for N-methyl amino acids dipeptide models, are depicted by red dotted circles. The structures of N-methyl alanine dipeptide of energy barriers A ((ϕ, ψ) = (150, 45)) and B ((ϕ, ψ) = (165, −165)) are shown in (E) and (F), respectively. In panels (E) and (F), dipeptides are drawn by stick (upper) and sphere (lower) models from the same direction, and contact regions are depicted by red dotted circles in sphere models.

force field with CMAP showed a wide distribution of open and closed structures (Figure 4C). Thus, the results for chcl3-w-CMAP indicated that the closed structure of CsA was stable in chloroform. In the solution NMR of CsA in chloroform, four singlet peaks from the amide proton region were observed in the spectrum, which indicated the presence of one major conformation of CsA [14]. This experimental result is consistent with the results for chcl3-w-CMAP. In contrast, the conformations in chcl3-wo-CMAP were widely distributed from the closed to the open structure on the PC1-PC2 plane (Figure 4B). Six structural clusters were observed in chcl3-wo-CMAP (Figure S10). This wide conformational distribution in chcl3-wo-CMAP is inconsistent with the NMR results, indicating a single conformation in chloroform.

The NOE signals of the NMR measurement of CsA in chloroform were compared with the atomic distances in chcl3-w-CMAP and chcl3-wo-CMAP [13]. The NOE signals separated for three or more amino acids (inter-cycle distances) were used for comparison. The number of NOE violations of 1 Å or more was four and three out of 13 for chcl3-w-CMAP and
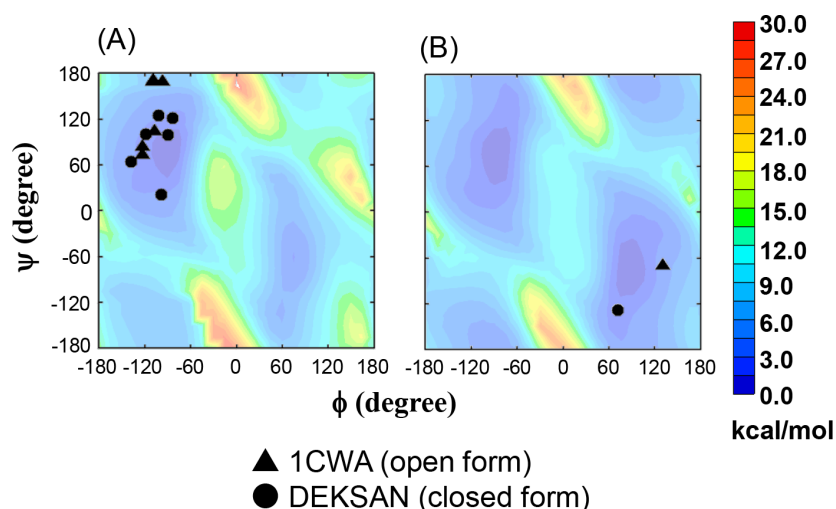
Figure 3 The (ϕ, ψ) angles of N-methyl amino acids in the crystal structures of cyclosporin A overlaid with the free-energy landscapes of N-methyl alanine and glycine. The conformations of N-methyl amino acids except for N-methyl glycine (A) and N-methyl glycine (Sarcosine) (B). the energy surfaces of N-methyl alanine and glycine are depicted. The residues in the open form [PDB ID: 1CWA] and closed form [CDC ID: DEKSAN] are depicted by triangles and circles, respectively.
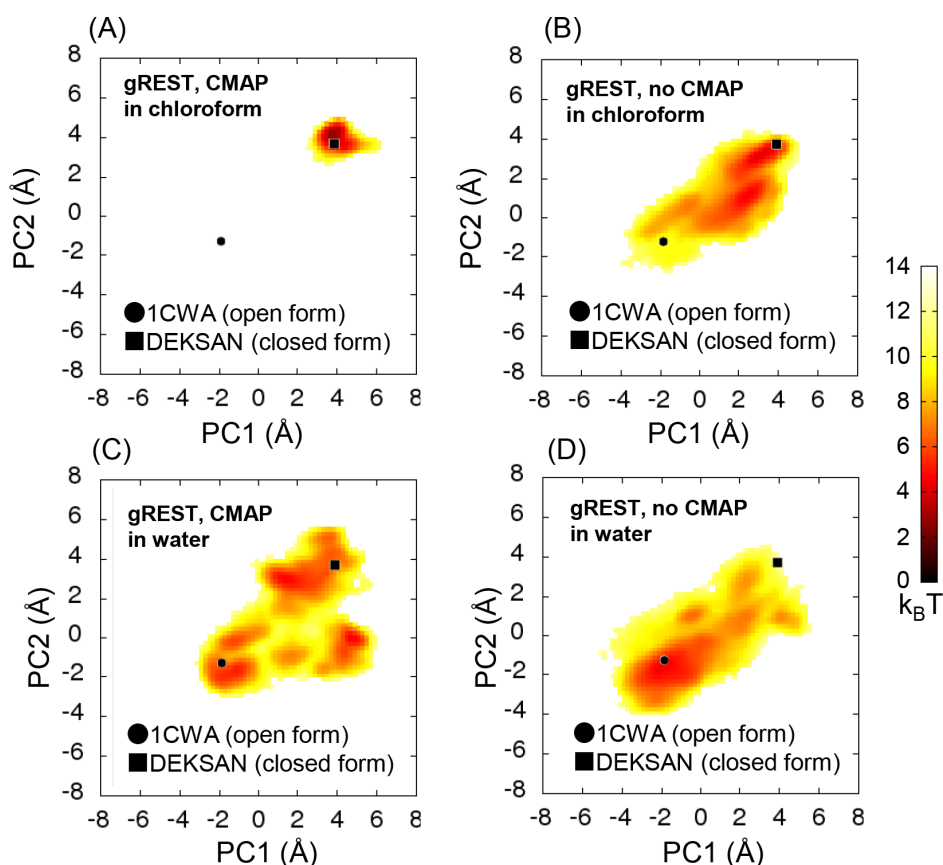

Figure 4 Free-energy landscape from gREST samplings in chloroform and water on the principal component space spanned by PC1 and PC2 axes. In panels (A) and (B), the results of gREST simulations in chloroform solution by using CHARMM force field with and without the CMAP term of N-methyl amino acids are shown, respectively. In panels (C) and (D), the results of gREST sampling in water by using CHARMM force field with and without the CMAP term for N-methyl amino acids are shown, respectively. The crystal structure of the open form [PDB ID: 1CWA] and closed form [CDC ID: DEKSAN] are shown by a black circle and a black square, respectively.

chcl3-wo-CMAP, respectively, suggesting that the numbers of NOE violations both with and without CMAP were small. Considering the clear difference in structural distribution with and without CMAP, as discussed above, NOE violations may not be appropriate to distinguish the structural distributions with and without CMAP.

gREST Simulations for CsA in Water

Next, gREST simulations for CsA in water were performed with and without the CMAP terms for the N-methyl amino acids, which are referred to as water-w-CMAP and water-wo-CMAP, respectively. In both water-w-CMAP and water-wo-CMAP, PCA results indicated that the conformations of CsA in water varied widely from the closed to the open structure (Figure 4C and 4D).

The free-energy landscape of water-w-CMAP was more complicated than that of water-wo-CMAP (Figure 4C). In water-w-CMAP, 12 structural clusters were found (Figure S11). Clusters 1 and 12 (PC1, PC2 ~ −2, −2) were close to the open crystal structure, whereas clusters 2, 3, 5, and 6 (PC1, PC2 ~ 3, 3) resembled the closed crystal structures. Clusters 4 and 7 were between the open and closed structures. In addition, skewed structures were observed in clusters 8, 9, and 10 (PC1, PC2 ~ 5, 0). In contrast, the free-energy landscape of water-wo-CMAP was rather simple (Figure 4D). The structures were widely distributed from the open to the closed structure, and the open structure appeared to be more stable than the closed structure in water-wo-CMAP (Figure S12).

Solution NMR studies have indicated that CsA has a variety of conformations in aqueous solutions. In the spectrum of the H/D exchange of CsA in acetonitrile [14], four singlet peaks derived from four amide protons were observed. These peaks widened as the proportion of water in the water-acetonitrile mixture increased. These results suggest that, whereas CsA adopts a single structure in a non-polar solvent, various conformations exist in water [14]. Accordingly, the free-energy landscapes calculated from the gREST simulations with CMAP suggest that, whereas a single closed structure was stable in chloroform, multiple stable conformations were found in water. In addition, the experiment by Ko et al. has shown that ~20% of closed-like structures are populated in a 1:1 methanol/water mixed solution, which is a highly polar solvent system such as water [53]. This suggests that the results of gREST with CMAP, which is a more stable closed-form structure, reproduces the results of actual NMR experiments.

To examine the capability of the structural sampling by gREST simulations, we performed comparisons of 1 μs conventional MD simulations of CsA from the open crystal structure [PDB ID: 1CWA] and the closed crystal structure [CDC ID: DEKSAN] in water using our force field. In the free-energy landscapes on the PCA space (PC1-PC2), the conventional MD simulations from the open crystal structure samples only open-like structures (Figure 5B). In contrast, in the conventional MD simulations of the closed crystal structure, two major basins corresponding to closed and skewed structures were observed (Figure 5A). All stable basins found in the conventional MD simulations were also observed in the gREST simulations. However, in conventional MD simulations, the open-like and closed-like structures did not convert to each other within 1 μs. Therefore, longer simulations are needed to achieve transition between the open and closed structures. On the other hand, the gREST simulations for 0.5 μs were capable of sampling the transition between open and closed structures.
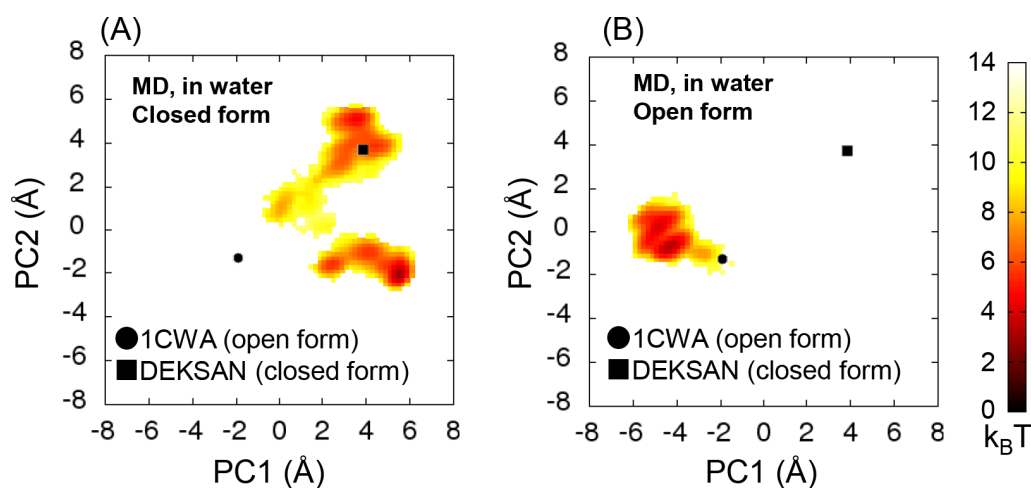

Figure 5 Free-energy landscape obtained from the conventional MD simulations in water on the principal component space spanned by PC1 and PC2 axis. (A) Results of 1 μs conventional MD simulations from the closed form [CDC ID: DEKSAN] and (B) open form [PDB ID: 1CWA]. The crystal structure of the open form [PDB ID: 1CWA] and closed form [CDC ID: DEKSAN] are shown by a black circle and a black square, respectively.

The free-energy landscape obtained from the conventional MD simulation for the closed form indicated that no structures close to the open form were sampled beyond the point around (PC1, PC2) = (0, 0) (Figure 5A). In addition, the results of the free-energy landscapes in the three gREST calculations, in which open and closed conformations were sampled (water-w-CMAP, water-wo-CMAP, and chcl3-wo-CMAP), showed a free-energy barrier around (PC1, PC2) = (0, 0) (Figure 4). Therefore, the position around (PC1, PC2) = (0, 0) was considered to be the energy barrier between the closed and open structures of CsA. The heights of the energy barrier were estimated from the free-energy landscapes of water-w-CMAP, water-wo-CMAP, and chcl3-wo-CMAP to be ~7.2 kcal/mol, ~5.4 kcal/mol, and ~5.4 kcal/mol at 300 K, respectively. In chcl3-w-CMAP, the free-energy barrier between the open and closed structures could not be estimated because only closed structures were sampled. However, we speculated that this energy barrier in chloroform was higher than that in water.

In summary, the barrier between the open and closed structures of CsA in water was significantly different from that in chloroform. The main reason for the difference was that the hydration made CsA more flexible in water. In contrast, the intramolecular hydrogen bonds in CsA were more stable in the nonpolar solvent. Furthermore, a quantum chemical study has shown that the energy barrier between *cis* and *trans* forms of the dihedral angle ω of the peptide bond in N-methylamino acid is lower in water than in hydrophobic solvents [21]. In CsA, the dihedral angle ω of the peptide bond between MLE2-MLE3 is *trans* and *cis* in the open and closed structures, respectively. The potential energy change of the dihedral also contributes to the change in the energy barrier between the open and closed structures.

Dihedral Angle ω of N-methyl amino acids

One of the important differences between the open and closed forms of CsA is the dihedral angle ω of the peptide bond between specific N-methyl amino acids, MLE2 and MLE3, which assumes the *trans* and *cis* state in the open and the closed structure, respectively. Here, this ω angle is referred to as "ω2" and other ω angle abbreviations are shown in Figures S1–S4. In the conventional MD simulations of CsA in water using the CHARMM force field for CsA developed in this study, the ω2 angle maintained the initial angle for 1 µs without *cis–trans* transition (Figures S5B and S6B). In contrast, in gREST in water, ω2 assumed both the *trans* and *cis* form with or without the CMAP of N-methyl amino acids (Figures S1B and S2B). In chloroform, the ω2 angles of gREST simulations with CMAP were *cis* (Figure S3B), whereas ω2 angles without CMAP were ~5% *trans* (Figure S4B).

We compared these conformations with the ω2 *cis* and *trans* states on the free-energy landscapes from gREST with CMAP of N-methyl amino acids (Figures S7 and S8). In both water and chloroform, conformations with ω2 *cis* were only found in the region of the closed structure (Figure S7A and S7B). In contrast, conformations with ω2 *trans* were observed in both the open and closed structures (Figure S7C). This means that the closed conformations are adopted in both the ω2 *cis* and *trans* states, whereas ω2 *trans* is required to form the open structure. On the other hand, regardless of the water and chloroform solvent, in the gREST without CMAP of N-methyl amino acids, this relationship disappears, and even if ω2 is in *cis*, the open structure appears (Figure S8). These results suggest that the CMAP terms of N-methyl amino acids also affect ω2 *cis–trans* transitions. In all simulations, the ω angles of N-methyl amino acids, other than ω2, were *trans* and did not change to *cis* (Figures S1–S6). In accordance with the crystal closed structure of CsA, only the ω angle between MLE2 and MLE3 undergoes *cis–trans* transitions.

Intramolecular Hydrogen Bonds in CsA

In a hydrophobic environment, CsA is expected to form intramolecular hydrogen bonds. In gREST with CMAP in chloroform, the average number of hydrogen bonds in CsA was 1.7 (1.6 for backbone hydrogen bonds) (Table S1). Compared to the four hydrogen bonds observed in the crystal closed structure [CDC ID: DEKSAN], two hydrogen bonds were broken, possibly owing to the dynamic behavior of CsA in solution (Figure S13A and S13B). In gREST without CMAP in chloroform, open and intermediate structures appeared in addition to the closed structures. In open and intermediate structures (clusters 1–4), the number of hydrogen bonds was 0.21–0.81, which was less than the average number of hydrogen bonds. In the closed clusters 5 and 6, the numbers of hydrogen bonds were 2.9 and 1.7, respectively. In water, regardless of whether CMAP of N-methyl amino acids was used, few intramolecular hydrogen bonds were observed, suggesting that the polar atoms in CsA formed hydrogen bonds with water.

Expected Conformational Changes of CsA During Membrane Permeation

Based on the findings of this study, the possible mechanism of CsA membrane permeation is as follows. First, in the aqueous phase, a wide range of structures from the open to the closed form appeared, accompanied by *cis–trans* exchanges in the ω angle of MLE2-MLE3. When CsA passes across the membrane, CsA adopts a single closed structure with intramolecular hydrogen bonds. In computer simulation studies on the membrane permeation of CsA conducted so far, their findings are consistent with our results [13,14,24,27].

Witek et al. compared a variety of conformations obtained from MSM analysis of MD simulations of CsA in water and chloroform and showed that many open conformations of CsA exist in chloroform [13]. This result is close to the findings

of our study without CMAP (chcl3-wo-CMAP), consistent with the fact that cross terms, such as CMAP, were not used in the MD simulations of MSM analysis. The single conformation of CsA in chloroform observed in our gREST with CMAP of N-methyl amino acids suggests the importance of the cross terms of backbone angles (ϕ/ψ) for peptide conformations.

Conclusion

In this study, we developed a CHARMM force field for CsA to which the cell membrane exhibits high membrane permeability despite its high molecular weight. In particular, we developed the CMAP terms for N-methyl amino acids, which are crucial for describing CsA backbone dynamics. It was shown that the energy surface E (ϕ, ψ) of N-methyl amino acid is different from that of ordinary amino acids. In particular, the stable region of the C5 sheet region disappeared, and a high-energy barrier was observed. This is due to the steric hindrance arising from the presence of the modified methyl group in the amide group of the main chain.

To verify the developed force field, we performed conventional MD and gREST simulations in chloroform and water. As a result, the CMAP terms for N-methyl amino acids largely affected the conformation of CsA in both chloroform and water. In particular, the results of gREST with CMAP for N-methyl amino acids were consistent with the solution NMR experiments. In chloroform, the closed conformation of CsA was observed exclusively, whereas in water multiple conformations ranging from the open to the closed conformation were observed. On the basis of these findings, the possible mechanism of CsA membrane permeation was predicted. In the aqueous phase, a wide range of structures from the open to the closed form appear, accompanied by *cis–trans* transitions in the ω angle of MLE2-MLE3. When CsA passes across the membrane, CsA adopts the closed structure with intramolecular hydrogen bonds. Our theory is consistent with those suggested by other computer simulation studies on the membrane permeation of CsA.

From a methodological point of view, the gREST method was efficient for conformational sampling. In particular, the time scales of *cis–trans* transitions in the ω angles of peptide bonds are much longer than the time scales of the conventional MD. In contrast, as shown in this study, the gREST simulations are capable of sampling *cis–trans* transitions of the ω angles, indicating that the gREST method is appropriate for simulations of CsA. In the future, we plan to simulate the direct transitions of CsA across membranes using the developed force field.

Conflict of Interest

T.Y., T.E., and M.I declare that they have no conflict of interest.

Author Contributions

T.Y. performed the calculations and analyses. T.Y., T.E., and M.I. discussed the results and wrote the paper.

Acknowledgements

References

[1] Tamamura, H., Kobayakawa, T., Ohashi, N. Mid-size drugs based on peptides and peptidomimetics: A new drug category. SpringerBriefs in Pharmaceutical Science & Drug Development (Springer, Singapore, 2018). https://doi.org/10.1007/978-981-10-7691-6

[2] Ruegger, A., Kuhn, M., Lichti, H., Loosli, H. R., Huguenin, R., Quiquerez, C., et al. Cyclosporin A, a peptide metabolite from Trichoderma polysporum (Link ex Pers.) Rifai, with a remarkable immunosuppressive activity. Helv. Chim. Acta 59, 1075-1092 (1976). https://doi.org/10.1002/hlca.19760590412

[3]   Wenger, R. M. Synthesis of cyclosporine and analogs - structural requirements for immunosuppressive activity. Angew. Chem. Int. Ed. Engl. 24, 77-85 (1985). https://doi.org/10.1002/anie.198500773

[4]   Hiestand, P. C., Gubler, H. U. Cyclosporins: Immunopharmacologic properties of natural cyclosporins. in The Pharmacology of Lymphocytes. (Bray, M. A., Morley, J. eds.), pp. 487-502 (Springer Berlin Heidelberg, Berlin, Heidelberg, 1988).

[5]   Liu, J., Farmer, J. D., Jr., Lane, W. S., Friedman, J., Weissman, I., Schreiber, S. L. Calcineurin is a common target of cyclophilin-cyclosporin A and FKBP-FK506 complexes. Cell 66, 807-815 (1991). https://doi.org/10.1016/0092-8674(91)90124-h

[6]   Liu, J., Albers, M. W., Wandless, T. J., Luan, S., Alberg, D. G., Belshaw, P. J., et al. Inhibition of T cell signaling by immunophilin-ligand complexes correlates with loss of calcineurin phosphatase activity. Biochemistry 31, 3896-3901 (1992). https://doi.org/10.1021/bi00131a002

[7]   Mikol, V., Kallen, J., Pflugl, G., Walkinshaw, M. D. X-ray structure of a monomeric cyclophilin A-cyclosporin A crystal complex at 2.1 A resolution. J. Mol. Biol. 234, 1119-1130 (1993). https://doi.org/10.1006/jmbi.1993.1664

[8]   Fesik, S. W., Gampe, R. T., Jr., Holzman, T. F., Egan, D. A., Edalji, R., Luly, J. R., et al. Isotope-edited NMR of cyclosporin A bound to cyclophilin: Evidence for a trans 9,10 amide bond. Science 250, 1406-1409 (1990). https://doi.org/10.1126/science.2255910

[9]   Weber, C., Wider, G., von Freyberg, B., Traber, R., Braun, W., Widmer, H., et al. The NMR structure of cyclosporin A bound to cyclophilin in aqueous solution. Biochemistry 30, 6563-6574 (1991). https://doi.org/10.1021/bi00240a029

[10] Fesik, S. W., Neri, P., Meadows, R., Olejniczak, E. T., Gemmecker, G. A model of the cyclophilin/cyclosporin A (CSA) complex from NMR and X-ray data suggests that CSA binds as a transition-state analog. J. Am. Chem. Soc. 114, 3165-3166 (1992). https://doi.org/10.1021/ja00034a087

[11] Kofron, J. L., Kuzmic, P., Kishore, V., Gemmecker, G., Fesik, S. W., Rich, D. H. Lithium chloride perturbation of cis-trans peptide bond equilibria: Effect on conformational equilibria in cyclosporin A and on time-dependent inhibition of cyclophilin. J. Am. Chem. Soc. 114, 2670-2675 (1992). https://doi.org/10.1021/ja00033a047

[12] Loosli, H.-R., Kessler, H., Oschkinat, H., Weber, H.-P., Petcher, T. J., Widmer, A. Peptide conformations. Part 31. The conformation of cyclosporin a in the crystal and in solution. Helv. Chim. Acta 68, 682-704 (1985). https://doi.org/10.1002/hlca.19850680319

[13] Witek, J., Keller, B. G., Blatter, M., Meissner, A., Wagner, T., Riniker, S. Kinetic models of cyclosporin A in polar and apolar environments reveal multiple congruent conformational States. J. Chem. Inf. Model. 56, 1547-1562 (2016). https://doi.org/10.1021/acs.jcim.6b00251

[14] Wang, C. K., Swedberg, J. E., Harvey, P. J., Kaas, Q., Craik, D. J. Conformational flexibility is a determinant of permeability for cyclosporin. J. Phys. Chem. B 122, 2261-2276 (2018). https://doi.org/10.1021/acs.jpcb.7b12419

[15] Schrodinger, LLC The PyMOL Molecular Graphics System, Version 1.8. (2015).

[16] Rezai, T., Bock, J. E., Zhou, M. V., Kalyanaraman, C., Lokey, R. S., Jacobson, M. P. Conformational flexibility, internal hydrogen bonding, and passive membrane permeability: Successful in silico prediction of the relative permeabilities of cyclic peptides. J. Am. Chem. Soc. 128, 14073-14080 (2006). https://doi.org/10.1021/ja063076p

[17] Rezai, T., Yu, B., Millhauser, G. L., Jacobson, M. P., Lokey, R. S. Testing the conformational hypothesis of passive membrane permeability using synthetic cyclic peptide diastereomers. J. Am. Chem. Soc. 128, 2510-2511 (2006). https://doi.org/10.1021/ja0563455

[18] Biron, E., Chatterjee, J., Ovadia, O., Langenegger, D., Brueggen, J., Hoyer, D., et al. Improving oral bioavailability of peptides by multiple N-methylation: Somatostatin analogues. Angew. Chem. Int. Ed. Engl. 47, 2595-2599 (2008). https://doi.org/10.1002/anie.200705797

[19] White, T. R., Renzelman, C. M., Rand, A. C., Rezai, T., McEwen, C. M., Gelev, V. M., et al. On-resin N-methylation of cyclic peptides for discovery of orally bioavailable scaffolds. Nat. Chem. Biol. 7, 810-817 (2011). https://doi.org/10.1038/nchembio.664

[20] Ahlbach, C. L., Lexa, K. W., Bockus, A. T., Chen, V., Crews, P., Jacobson, M. P., et al. Beyond cyclosporine A: conformation-dependent passive membrane permeabilities of cyclic peptide natural products. Future Med. Chem. 7, 2121-2130 (2015). https://doi.org/10.4155/fmc.15.78

[21] Md. Abdur Rauf, S., Arvidsson, P. I., Albericio, F., Govender, T., Maguire, G. E. M., Kruger, H. G., et al. The effect of N-methylation of amino acids (Ac-X-OMe) on solubility and conformation: A DFT study. Org. Biomol. Chem. 13, 9993-10006 (2015). https://doi.org/10.1039/C5OB01565K

[22] Shinoda, W. Permeability across lipid membranes. Biochim. Biophys. Acta 1858, 2254-2265 (2016). https://doi.org/10.1016/j.bbamem.2016.03.032

[23] Dickson, C. J., Hornak, V., Bednarczyk, D., Duca, J. S. Using membrane partitioning simulations to predict permeability of forty-nine drug-like molecules. J. Chem. Inf. Model. 59, 236-244 (2019). https://doi.org/10.1021/acs.jcim.8b00744

[24] Witek, J., Muhlbauer, M., Keller, B. G., Blatter, M., Meissner, A., Wagner, T., et al. Interconversion rates between conformational states as rationale for the membrane permeability of Cyclosporines. Chemphyschem 18, 3309-3314 (2017). https://doi.org/10.1002/cphc.201700995

[25] Witek, J., Wang, S., Schroeder, B., Lingwood, R., Dounas, A., Roth, H. J., et al. Rationalization of the membrane permeability differences in a series of analogue cyclic decapeptides. J. Chem. Inf. Model. 59, 294-308 (2019). https://doi.org/10.1021/acs.jcim.8b00485

[26] Ono, S., Naylor, M. R., Townsend, C. E., Okumura, C., Okada, O., Lee, H. W., et al. Cyclosporin A: Conformational complexity and chameleonicity. J. Chem. Inf. Model. 61, 5601-5613 (2021). https://doi.org/10.1021/acs.jcim.1c00771

[27] Sugita, M., Sugiyama, S., Fujie, T., Yoshikawa, Y., Yanagisawa, K., Ohue, M., et al. Large-scale membrane permeability prediction of cyclic peptides crossing a lipid bilayer based on enhanced sampling molecular dynamics simulations. J. Chem. Inf. Model. 61, 3681-3695 (2021). https://doi.org/10.1021/acs.jcim.1c00380

[28] Mackerell, A. D., Jr., Feig, M., Brooks, C. L., 3rd. Extending the treatment of backbone energetics in protein force fields: Limitations of gas-phase quantum mechanics in reproducing protein conformational distributions in molecular dynamics simulations. J. Comput. Chem. 25, 1400-1415 (2004). https://doi.org/10.1002/jcc.20065

[29] Mirijanian, D. T., Mannige, R. V., Zuckermann, R. N., Whitelam, S. Development and use of an atomistic CHARMM-based forcefield for peptoid simulation. J. Comput. Chem. 35, 360-370 (2014). https://doi.org/10.1002/jcc.23478

[30] Weiser, L. J., Santiso, E. E. A CGenFF-based force field for simulations of peptoids with both cis and trans peptide bonds. J. Comput. Chem. 40, 1946-1956 (2019). https://doi.org/10.1002/jcc.25850

[31] Kamiya, M., Sugita, Y. Flexible selection of the solute region in replica exchange with solute tempering: Application to protein-folding simulations. J. Chem. Phys. 149, 072304 (2018). https://doi.org/10.1063/1.5016222

[32] Best, R. B., Zhu, X., Shim, J., Lopes, P. E., Mittal, J., Feig, M., et al. Optimization of the additive CHARMM all-atom protein force field targeting improved sampling of the backbone phi, psi and side-chain chi(1) and chi(2) dihedral angles. J. Chem. Theory Comput. 8, 3257-3273 (2012). https://doi.org/10.1021/ct300400x

[33] Vanommeslaeghe, K., Hatcher, E., Acharya, C., Kundu, S., Zhong, S., Shim, J., et al. CHARMM general force field: A force field for drug-like molecules compatible with the CHARMM all-atom additive biological force fields. J. Comput. Chem. 31, 671-690 (2010). https://doi.org/10.1002/jcc.21367

[34] Vanommeslaeghe, K., MacKerell, A. D., Jr. Automation of the CHARMM General Force Field (CGenFF) I: Bond perception and atom typing. J. Chem. Inf. Model. 52, 3144-3154 (2012). https://doi.org/10.1021/ci300363c

[35] Vanommeslaeghe, K., Raman, E. P., MacKerell, A. D., Jr. Automation of the CHARMM General Force Field (CGenFF) II: Assignment of bonded parameters and partial atomic charges. J. Chem. Inf. Model. 52, 3155-3168 (2012). https://doi.org/10.1021/ci3003649

[36] Yu, W., He, X., Vanommeslaeghe, K., MacKerell, A. D., Jr. Extension of the CHARMM General Force Field to sulfonyl-containing compounds and its utility in biomolecular simulations. J. Comput. Chem. 33, 2451-2468 (2012). https://doi.org/10.1002/jcc.23067

[37] Soteras Gutierrez, I., Lin, F. Y., Vanommeslaeghe, K., Lemkul, J. A., Armacost, K. A., Brooks, C. L., 3rd, et al. Parametrization of halogen bonds in the CHARMM general force field: Improved treatment of ligand-protein interactions. Bioorg. Med. Chem. 24, 4812-4825 (2016). https://doi.org/10.1016/j.bmc.2016.06.034

[38] Frisch, M. J., Trucks, G. W., Schlegel, H. B., Scuseria, G. E., Robb, M. A., Cheeseman, J. R., et al. Gaussian 09, Revision A.02 (Gaussian, Inc., Wallingford CT, 2016).

[39] Shao, Y., Gan, Z., Epifanovsky, E., Gilbert, A. T. B., Wormit, M., Kussmann, J., et al. Advances in molecular quantum chemistry contained in the Q-Chem 4 program package. Mol. Phys. 113, 184-215 (2015). https://doi.org/10.1080/00268976.2014.952696

[40] Halkier, A., Helgaker, T., Jørgensen, P., Klopper, W., Koch, H., Olsen, J., et al. Basis-set convergence in correlated calculations on Ne, N2, and H2O. Chem. Phys. Lett. 286, 243-252 (1998). https://doi.org/10.1016/S0009-2614(98)00111-0

[41] Liu, P., Kim, B., Friesner, R. A., Berne, B. J. Replica exchange with solute tempering: a method for sampling biological systems in explicit water. Proc. Natl. Acad. Sci. U.S.A. 102, 13749-13754 (2005). https://doi.org/10.1073/pnas.0506346102

[42] Wang, L., Friesner, R. A., Berne, B. J. Replica exchange with solute scaling: a more efficient version of replica exchange with solute tempering (REST2). J. Phys. Chem. B 115, 9431-9438 (2011). https://doi.org/10.1021/jp204407d

[43] Kobayashi, C., Jung, J., Matsunaga, Y., Mori, T., Ando, T., Tamura, K., et al. GENESIS 1.1: A hybrid-parallel molecular dynamics simulator with enhanced sampling algorithms on multiple computational platforms. J. Comput. Chem. 38, 2193-2206 (2017). https://doi.org/10.1002/jcc.24874

[44] Jung, J., Mori, T., Kobayashi, C., Matsunaga, Y., Yoda, T., Feig, M., et al. GENESIS: A hybrid-parallel and multi-

scale molecular dynamics simulator with enhanced sampling algorithms for biomolecular and cellular simulations. Wiley Interdiscip. Rev. Comput. Mol. Sci. 5, 310-323 (2015). https://doi.org/10.1002/wcms.1220

[45] Jo, S., Kim, T., Iyer, V. G., Im, W. CHARMM-GUI: A web-based graphical user interface for CHARMM. J. Comput. Chem. 29, 1859-1865 (2008). https://doi.org/10.1002/jcc.20945

[46] Lee, J., Cheng, X., Swails, J. M., Yeom, M. S., Eastman, P. K., Lemkul, J. A., et al. CHARMM-GUI input generator for NAMD, GROMACS, AMBER, OpenMM, and CHARMM/OpenMM simulations using the CHARMM36 additive force field. J. Chem. Theory Comput. 12, 405-413 (2016). https://doi.org/10.1021/acs.jctc.5b00935

[47] Huang, J., Rauscher, S., Nawrocki, G., Ran, T., Feig, M., de Groot, B. L., et al. CHARMM36m: An improved force field for folded and intrinsically disordered proteins. Nat. Methods 14, 71-73 (2017). https://doi.org/10.1038/nmeth.4067

[48] Jorgensen, W. L., Chandrasekhar, J., Madura, J. D., Impey, R. W., Klein, M. L. Comparison of simple potential functions for simulating liquid water. J. Chem. Phys. 79, 926-935 (1983). https://doi.org/10.1063/1.445869

[49] Dietz, W., Heinzinger, K. A Molecular Dynamics study of liquid chloroform. Berichte der Bunsengesellschaft für physikalische Chemie 89, 968-977 (1985). https://doi.org/10.1002/bbpc.19850890909

[50] Mayne, C. G., Saam, J., Schulten, K., Tajkhorshid, E., Gumbart, J. C. Rapid parameterization of small molecules using the Force Field Toolkit. J. Comput. Chem. 34, 2757-2770 (2013). https://doi.org/10.1002/jcc.23422

[51] Abraham, M. J., Murtola, T., Schulz, R., Páll, S., Smith, J. C., Hess, B., et al. GROMACS: High performance molecular simulations through multi-level parallelism from laptops to supercomputers. SoftwareX 1-2, 19-25 (2015). https://doi.org/10.1016/j.softx.2015.06.001

[52] Brooks, C., Case, D. A. Simulations of peptide conformational dynamics and thermodynamics. Chem. Rev. 93, 2487-2502 (1993). https://doi.org/10.1021/cr00023a008

[53] Ko, S. Y., Dalvit, C. Conformation of cyclosporin A in polar solvents. Int. J. Pept. Protein Res. 40, 380-382 (1992). https://doi.org/10.1111/j.1399-3011.1992.tb00314.x